

Using remotely-sensed estimates of soil moisture to infer soil texture and hydraulic properties across a semi-arid watershed

Joseph A. Santanello Jr.^{a,b,*}, Christa D. Peters-Lidard^b, Matthew E. Garcia^{b,c},
David M. Mocko^{b,d}, Michael A. Tischler^e, M. Susan Moran^f, D.P. Thoma^f

^a Earth System Science Interdisciplinary Center, UMCP, College Park, MD, United States

^b NASA-GSFC Hydrological Sciences Branch, Greenbelt, MD, United States

^c Goddard Earth Sciences and Technology Center, UMBC, Baltimore, MD, United States

^d Science Applications International Corporation, McLean, VA, United States

^e U.S. Army Engineer Research and Development Center, TEC, Alexandria, VA, United States

^f USDA ARS Southwest Watershed Research Center, Tucson, AZ, United States

Received 10 October 2006; received in revised form 15 January 2007; accepted 3 February 2007

Abstract

Near-surface soil moisture is a critical component of land surface energy and water balance studies encompassing a wide range of disciplines. However, the processes of infiltration, runoff, and evapotranspiration in the vadose zone of the soil are not easy to quantify or predict because of the difficulty in accurately representing soil texture and hydraulic properties in land surface models. This study approaches the problem of parameterizing soil properties from a unique perspective based on components originally developed for operational estimation of soil moisture for mobility assessments. Estimates of near-surface soil moisture derived from passive (L-band) microwave remote sensing were acquired on six dates during the Monsoon '90 experiment in southeastern Arizona, and used to calibrate hydraulic properties in an offline land surface model and infer information on the soil conditions of the region. Specifically, a robust parameter estimation tool (PEST) was used to calibrate the Noah land surface model and run at very high spatial resolution across the Walnut Gulch Experimental Watershed. Errors in simulated versus observed soil moisture were minimized by adjusting the soil texture, which in turn controls the hydraulic properties through the use of pedotransfer functions. By estimating within a continuous range of widely applicable soil properties such as sand, silt, and clay percentages rather than applying rigid soil texture classes, lookup tables, or large parameter sets as in previous studies, the physical accuracy and consistency of the resulting soils could then be assessed.

In addition, the sensitivity of this calibration method to the number and timing of microwave retrievals is determined in relation to the temporal patterns in precipitation and soil drying. The resultant soil properties were applied to an extended time period demonstrating the improvement in simulated soil moisture over that using default or county-level soil parameters. The methodology is also applied to an independent case at Walnut Gulch using a new soil moisture product from active (C-band) radar imagery with much lower spatial and temporal resolution. Overall, results demonstrate the potential to gain physically meaningful soil information using simple parameter estimation with few but appropriately timed remote sensing retrievals.

© 2007 Elsevier Inc. All rights reserved.

Keywords: Parameter estimation; Soil moisture; Active microwave; Passive microwave; PBMR; Land surface modeling; Model calibration; Soil hydraulic properties; Temporal sampling; Watershed modeling; Soil type; Pedotransfer functions

1. Introduction

Soil moisture remains an essential yet elusive component of Earth system science research across a wide range of scales and applications. In addition to impacting agriculture, water resource management, and extreme events such as flooding and drought, the day-to-day variability in soil moisture on field

* Corresponding author. Earth System Science Interdisciplinary Center, UMCP, College Park, MD, United States. Tel.: +1 301 286 7450.

E-mail address: sntnello@hsb.gsfc.nasa.gov (J.A. Santanello).

to global scales is an important quantity for atmospheric modeling and prediction. In fact, the accuracies of climate, mesoscale, boundary layer, land surface, and hydrologic models are ultimately dependent on proper treatment and simulation of the state and transfer of water and heat at the land surface (Betts, 2000; Betts et al., 2003; Berbery et al., 2003; Findell & Eltahir, 2003; Koster, 2004).

Unfortunately, soil moisture is not as easily measured or observed as atmospheric properties such as temperature, humidity, and wind speed. For example, in-situ or remotely-sensed observations of soil moisture for initialization, update, and validation purposes are not yet available on the scales of most models. Observations are generally confined to short-term field experiments, many of which have highlighted the heterogeneous nature of soils in terms of water content and texture (Mohanty et al., 2002). Indirect estimates of soil moisture can be obtained using thermal infrared measurements (Carlson et al., 1995), but require a priori information on the surface characteristics. As an alternative, passive and active microwave remote sensing methods have had the greatest success in estimating soil moisture in a temporally and spatially consistent manner (Hollenbeck et al., 1996; Moran et al., 2004; Thoma et al., 2006).

Recent studies have noted that the most successful and promising approach to estimating soil moisture continuously over time and space must include a combination of remote sensing and modeling (Entekhabi et al., 1999; Houser et al., 1998). The majority of land surface models (LSMs) require soil hydraulic parameters to solve for the transport of moisture within the soil using Richards' (1931) formulations. These parameters are often derived from soil texture information, but due to the heterogeneous nature of soils and lack of detailed maps of soil properties, soil parameterization schemes are often crude, inflexible, or inappropriate. Further, LSM simulation of soil moisture can be more dependent upon the specification of hydraulic parameters than atmospheric forcing or surface conditions (Gutmann & Small, 2005; Pitman, 2003; Santanello & Carlson, 2001).

Because of these difficulties, numerous attempts have been made to optimize LSM parameters using observations of state variables such as soil moisture and surface temperature as constraints (Gupta et al., 1999; Hess, 2001; Hogue et al., 2005; Liu et al., 2004, 2005). While these studies highlight the potential for parameter estimation techniques to derive large sets of 'effective' parameters and diagnose specific model weaknesses, little has been gained in terms of acquiring physically meaningful or hydraulically consistent estimates of individual parameters. Because of the complexity and number of estimation techniques and parameter sets employed in these studies, it remains difficult to infer or derive any parameter information that could be applied to other independent studies or models.

With these issues in mind, this paper examines the potential use of passive and active microwave retrievals of near-surface soil moisture to calibrate an LSM and infer a physically meaningful and consistent set of soil hydraulic parameters, using a combination of high-resolution land surface modeling and parameter estimation. The experimental design of this work

was originally developed for the purpose of estimating troop and vehicle mobility for the United States Army based on operational soil moisture prediction from a very limited set of input data (Army Remote Moisture System; ARMS; Tischler et al., 2007). Here, we have tested and extended ARMS to assess the ability of parameter estimation techniques to minimize inherent model error, yet still provide information on difficult to obtain soil properties over the Walnut Gulch Experimental Watershed in Arizona.

Accordingly, Section 2 summarizes the current state of knowledge of the many components of the ARMS project including soil parameterizations in LSMs, microwave remote sensing of soil moisture, and parameter estimation. In Section 3, the models, site, and remote sensing data employed in this study are described. Results of the calibration experiments are presented in Section 4, including an evaluation of the optimized parameters and sensitivity to temporal sampling of remote sensing. Finally, Section 5 discusses the limitations and applicability of the results, including suggestions for the future utility of physically meaningful parameters in LSMs.

2. Background

2.1. Soil parameterizations in LSMs

The influence of near-surface soil moisture on the partitioning of surface turbulent fluxes from offline LSMs to fully coupled global climate models has been well-documented (e.g., Braun & Schadler, 2005; Cuenca et al., 1996; Ek & Cuenca, 1994; Ek & Holtslag, 2003; Jacobs & Debruin, 1992; Santanello & Carlson, 2001; Sun & Bosilovich, 1996). In order to simulate the evolution of moisture in the soil, a set of soil hydraulic parameters are combined with expressions (known as soil moisture characteristic curves) relating soil moisture (θ) with matric potential (ψ), and soil moisture with hydraulic conductivity (K). The expressions derived by Brooks and Corey (1964) and Campbell (1974) are most commonly used in meteorological coupled models, while the van Genuchten (1980) functions based on a different set of soil measurements are used for more detailed soil and hydrological models. A full description and evaluation of these functions can be found in Braun and Schadler (2005).

The three forms of the characteristic curves above depend on a set of 4 (Campbell, 1974) or 5 (Brooks & Corey, 1964; van Genuchten, 1980) hydraulic parameters, which are a function of the soil composition and structure. These parameters, which are difficult to measure or estimate in a consistent fashion, include the saturated matric potential (ψ_s ; aka "bubbling" or "air entry"), the saturated hydraulic conductivity (K_s), the saturated soil moisture content (porosity; θ_s), the residual soil moisture content (θ_r), and the pore size distribution index (b).

To acquire a somewhat standard set of parameters for LSM applications, 'bulk' parameters have been derived that are a function of soil type. The results of Clapp and Hornberger (hereafter CH; 1978), Rawls et al. (1982), and Cosby et al. (1984) provide the most extensive and commonly employed lookup tables of hydraulic parameters for LSMs, with atmospheric-based

applications favoring CH and Cosby and soil hydrology models employing the Rawls parameters. Unfortunately, parameter lookup tables are only as accurate as the available soil texture type information and provide an “average” value of each parameter for each soil type. High-resolution soil texture maps are difficult to obtain, particularly for regions outside the U. S. and on global scales, and there is little flexibility between soil types or for mixed soils despite findings that larger differences in soil properties have been observed within a soil type than between types (Feddes et al., 1993; Gutmann & Small, 2005; Soet & Stricker, 2003).

To bridge the gap between rigid soil textural classes and the heterogeneous nature of soils, numerous pedotransfer functions (PTFs) have been developed (Sobieraj et al., 2001). The most commonly used ‘class’ PTFs relate discrete soil types to hydraulic parameters and are the basis upon which lookup tables are used in LSMs and meteorological modeling applications. ‘Continuous’ PTFs are more detailed and relate measurable soil properties such as percent of sand and clay, porosity, and bulk density to hydraulic properties using regression equations derived from soil samples. These functions are continuous without bounds, and therefore allow more flexibility and independence in parameter values than those from lookup tables. More importantly, continuous PTFs that are able to reproduce a real averaged conditions in LSMs have been shown to scale linearly in space and therefore could be used to infer spatially-aggregated hydraulic parameters (Soet & Stricker, 2003). While the advantages of continuous over class PTFs have been demonstrated for hydrologic models, continuous PTFs are not routinely employed in LSMs or atmospheric models where the broad definition and application of soil types still dominate the simulation of soil moisture.

2.2. Parameter estimation

An alternative to specifying soil hydraulic parameters in LSMs is to use parameter estimation and model calibration techniques. For example, a relatively simple and well-established Parameter Estimation model (PEST; Doherty, 2004) has been used in a number of scientific disciplines to optimize model parameters given limited observations of fundamental output variables. For example, by adjusting soil porosity in an LSM until the difference in simulated versus observed soil moisture is minimized (through a specified objective function), an LSM can be calibrated using PEST.

Overall, the majority of parameter estimation studies have focused on large sets of parameters and complex algorithms that require a great deal of computational time (e.g. Hogue et al., 2005; Liu et al., 2003, 2004). From these studies, it could also be argued that the bulk of the work done to this point has been focused on ‘model calibration’ rather than estimating physically meaningful soil properties, particularly when there is significant model error accounted for in the optimized parameters. For example, Scott et al. (2000) performed soil hydraulic parameter estimation using a LSM in the Walnut Gulch Experimental Watershed (WGEW). While their results highlight the relative sensitivity of soil moisture simulations to individual hydraulic

parameters, they also stress that the derived parameters are ‘effective’ in nature, compensating for errors in the soil physics of the model, and that further research is needed to assess the potential for parameter estimation across spatially heterogeneous and distributed watersheds.

2.3. Remote sensing of soil moisture

Due to the limited nature of available soil instrumentation and measurement techniques (e.g., theta probe, Time Domain Reflectometry, Vitel probe, gravimetric), a spatially continuous and reliable network of soil moisture measurements that could be used to initialize and evaluate LSMs does not exist. As a result, passive microwave (L-band; 1.4 GHz) estimation of soil moisture has been explored using instruments such as NASA’s push-broom microwave radiometer (PBMR; Schmugge, 1998). Passive microwave radiometers flown on aircraft have shown a great deal of promise in estimating soil moisture across varying surface conditions due to the sensitivity of the dielectric constant (and therefore brightness temperature) to changes in water content within the top 5 cm of soil (Burke et al., 1997; Hollenbeck et al., 1996; Mattikalli et al., 1998; Schmugge, 1983).

More recently, techniques have been developed to estimate soil moisture using active microwave remote sensing (generally C-band; 5.3 GHz) with synthetic aperture radar (SAR) processing. Active sensors aboard satellite platforms can potentially provide high-resolution estimates of soil moisture when combined with empirical and physical models (Thoma et al., 2006). To date, there have been mixed results using radar remote sensing to estimate soil moisture due to the sensitivity of high frequency backscatter to the nature and degree of surface interactions and, consequently, the amount of signal correction required (see also review by Moran et al., 2004).

Recently, Thoma et al. (2006) have developed an image differencing technique for active remote sensing that shows promise in eliminating much of the noise in C-band radar data. This ‘delta index’ method requires a single reference (dry) image to compare with separate (wet) images over the same domain, assuming no other changes in surface characteristics between image acquisition dates. The delta index is defined as,

$$\text{delta index} = \left| \frac{\sigma_{\text{wet}} - \sigma_{\text{dry}}}{\sigma_{\text{dry}}} \right| \quad (1)$$

where σ_{dry} is the backscatter (db) from a dry radar image, and σ_{wet} is the radar backscatter (db) from the identical pixel location in a wet image, and has a near linear (1:1) relationship with volumetric soil moisture. Variability in soil moisture is captured through the relative change of backscatter between images, and therefore a unique estimate of soil moisture is acquired for every pixel on each wet image date. This method acts to minimize errors due to surface roughness effects using filtering techniques to reduce the amount of speckle that is common in radar imagery (particularly in regions of high coarse fraction), and is particularly applicable to semi-arid regions where a spatially-uniform dry reference image can be acquired (Thoma et al., 2006).

2.4. Estimation of soil hydraulic properties

There have been numerous efforts to estimate soil hydraulic properties using a combination of remote sensing imagery, LSMs, radiative transfer (emission) models, and observations. The work of van de Griend and O'Neill (1986) and Camillo et al. (1986) demonstrated that changes in soil moisture estimated from microwave (L-band) remote sensing could be related to the thermal inertia and hydrologic properties of the soil. While their results are valid only for a brief drydown period under highly-controlled conditions, they suggest that results may be improved by including a wider range of soil moisture conditions that capture the functional drying curves represented by the soil model parameterizations.

Following the work of Camillo et al. (1986), Burke et al. (1997), Burke et al. (1998) used a coupled land surface-microwave emission model in conjunction with radiometer measurements over a 10-day period to infer soil properties for bare and vegetated soil plots. Using this approach, hydraulic parameters were adjusted individually to match the emission model output with L-band radiometer measurements. Overall, these results point towards the future use of PTFs rather than a one-at-a-time parameter estimation approach to acquire spatially-distributed soil properties over watersheds, and suggest that an intensive period of microwave observations should be performed to capture significant soil drydown events.

Other 'combination' approaches to estimating soil properties have been tested that incorporate albedo and evaporation data (Feddes et al., 1993), but require a great deal of measurements and parameterizations thereby limiting their application to highly-controlled and plot-scale experiments. Image differencing techniques using L-band remote sensing to attribute changes in soil moisture to soil hydraulic properties have also been developed (Ahuja et al., 1993; Hollenbeck et al., 1996; Mattikalli et al., 1998). Their results demonstrate the strong qualitative relationships between microwave measurements and soil type and properties (e.g., K_{sat}), and confirm the theoretical framework by which a more comprehensive approach to estimating these parameters can be based.

2.5. Summary

Studies have demonstrated that the strong link between microwave remote sensing and soil moisture can provide a pathway to improve LSM soil physics and parameterizations. While these works have provided a strong physical and methodological foundation by which to address these issues, each has limitations in terms of scope and applicability that can now be improved upon by taking the suggested next steps and utilizing new approaches and data. Specifically, this paper will bridge the gaps between and extend previous studies by:

- 1) Determining the ability of parameter estimation to calibrate a LSM and to infer *physically meaningful estimates* of soil hydraulic properties using pedotransfer functions and microwave remote sensing of soil moisture at *high spatial and temporal resolution*;

- 2) Testing the sensitivity of the calibration process and retrieved properties to *precipitation* and *soil drydown* patterns using temporal sampling of airborne remote sensing imagery; and
- 3) Applying the retrieved soil parameters to an *independent dataset*, and assess the ability of a new image differencing technique of estimating soil moisture from *active satellite* microwave remote sensing to be used in the calibration process.

3. Methodology and data

3.1. ARMS background

The Army Remote Moisture System (ARMS; Tischler et al., 2007) project is an ongoing collaboration between the U. S. Army Corps of Engineers, U. S. Department of Agriculture, NASA's Goddard Space Flight Center, and the University of Wyoming. The goal of this work is to provide improved operational estimates of soil moisture and hydraulic properties as inputs to decision-making models based on factors such as troop and vehicle mobility and landing strip suitability. The three main components of ARMS are 1) *high-resolution microwave remote sensing* of soil moisture, used to 2) calibrate a *land surface model* by optimizing hydraulic properties through 3) *parameter estimation*. The ultimate goal of ARMS is to be able to use limited site information and radar-based soil moisture retrievals to calibrate an LSM for any location in the world and enable soil moisture and properties to be more accurately simulated in an analysis and forecast setting. While this study is focused on a semi-arid testbed in Arizona, ARMS is also being tested at other diverse locations across the U. S. (OK, GA, and CO).

3.2. Site information

The USDA Agricultural Research Service, Southwest Watershed Research Center, Walnut Gulch Experimental Watershed (WGEW) covers 150-km² in the San Pedro Valley of Southeastern Arizona and is dominated by semi-arid desert shrubs (<30% cover) and grasses (<50% cover). The detailed instrumentation and long record length of the datasets available in this region have made the WGEW the focus of many hydrological, meteorological, and remote sensing studies. Most notably, the Monsoon '90 field experiment (M90; Kustas et al., 1991) was conducted in this region in July and August of 1990, and included the deployment of eight Metflux sites across the watershed that measured standard meteorological data as well as land cover, soil moisture, and soil property information. (Fig. 1)

At each Metflux site, standard meteorological variables were measured at 20-minute intervals. Precipitation measurements were derived from a dense 98-gauge network covering the entire watershed, from which spatially interpolated rainfall estimates (useful for modeling applications) have been generated using a variety of techniques (Garcia et al., submitted for publication; Houser et al., 1998). Two supersites were furnished with additional instrumentation: Lucky Hills (LH) located in the

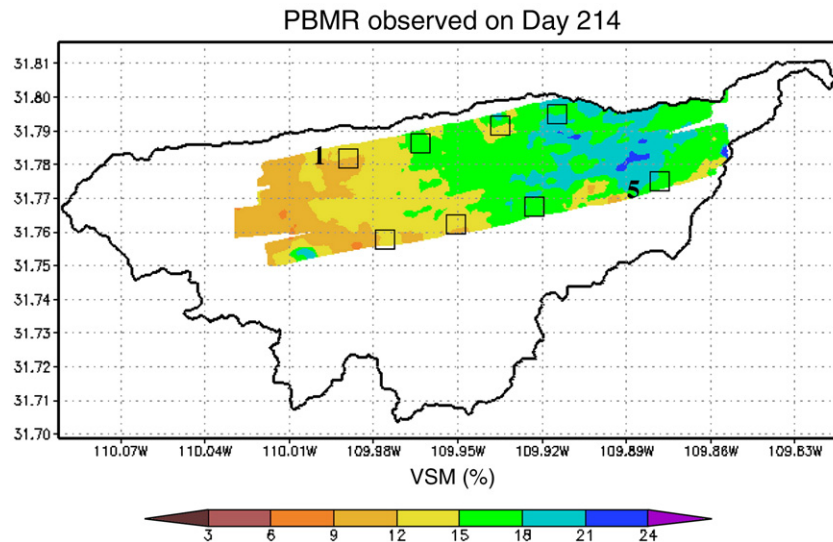


Fig. 1. The Walnut Gulch Experimental Watershed in southeastern Arizona (outlined in black) covers 148 km² and is heavily instrumented with meteorological, flux, and rain gauge data. The M90 experiment included 8 Metflux sites (□) of which Lucky Hills (Site 1) and Kendall (Site 5) were supersites. Overlain are estimates of volumetric soil moisture (m³ m⁻³ * 100) derived from push-broom microwave radiometer measurements on DOY 214.

shrub-dominated north-central part of the domain, and Kendall located in the grasslands of the east. Soil moisture in the upper 5 cm layer was estimated at each site using multiple gravimetric measurements, and vertical profiles of soil moisture were estimated at Kendall and LH using Time Domain Reflectometry, giving estimates from 5–50 cm in depth.

Overall, the conditions throughout the WGEW are dominated by the summer monsoon of July and August, when the bulk of the annual 250–500 mm rainfall (mainly convective) occurs. During the period from April–July, the soils often reach a desiccated state before the onset of the monsoonal precipitation. Rainfall events during the monsoon period are typically <10 mm and only influence the top 10 cm of soil before being quickly returned to the atmosphere within 3 days through evapotranspiration (Kurc & Small, 2004), thereby making the near-surface soil the dominant variable reservoir of moisture in this region.

3.3. Remote sensing of soil moisture

Passive microwave remote sensing measurements (L-band; 21-cm) of brightness temperature were made over a significant portion of the WGEW during the M90 experiment using NASA's push-broom microwave radiometer (PBMR), and are described in detail in Schmugge et al. (1994). From this dataset, six daily estimates of near-surface soil moisture are available both before (DOY 212) and after (DOY 214, 216, 217, 220, and 221) the onset of precipitation. The PBMR data was resampled to 40 m resolution and mapped to a UTM grid that covers a subset of the WGEW that includes all 8 Metflux sites. Schmugge et al. (1994) showed that brightness temperature measurements correlated well with both rainfall and 0–5 cm soil moisture measured at the sites. Fig. 2 shows the PBMR and gravimetric estimates of soil moisture at the Kendall and LH sites along with gauge-interpolated precipitation during the M90 period. These plots highlight the desiccated soil conditions

before the first and most intense rainfall event on DOY 213, and more importantly how the PBMR images capture the period of rapid soil drying thereafter.

For the 2002–4 period active, or radar, microwave remote sensing (C-band; 5.6 cm) measurements were acquired from RADARSAT-1 imagery. A reference (dry) image was taken on 19 January 2003 and combined with images during the monsoon period (29 July, 22 August, and 15 September 2003) to derive soil moisture using the delta index approach (Eq. (1)). The three resulting 0–5 cm soil moisture estimates cover a 6 week period spanning an extended (seasonal) drydown period immediately following rainfall. The nominal resolution of RADARSAT-1 is 7 m and covers the entire WGEW domain, but the raw backscatter data was further processed and filtered as discussed by Thoma et al. (2006) to 210 and 280 m resolution to reduce the effects of speckle.

3.4. LSM

The Noah land surface model (Chen et al., 1996; Ek et al., 2003) was originally developed from the land component of the Oregon State University 1-D planetary boundary layer model (OSU; Troen and Mahrt, 1984), and is currently employed as the land surface scheme in NCEP's operational version of the Weather Research and Forecasting nonhydrostatic Mesoscale Model (WRF-NMM). Noah has been used across a wide range of scales in both offline and coupled modes, and extensive evaluations and discussion of the Noah physics and comparisons to other LSMs has been performed by Robock et al. (2003), among others.

The offline version (2.6) of Noah was configured to run at 40 m resolution over the WGEW. Forcing data was acquired from the LH site and applied uniformly across the domain including downward shortwave and longwave radiation, air temperature, specific humidity, wind speed at a specified reference height

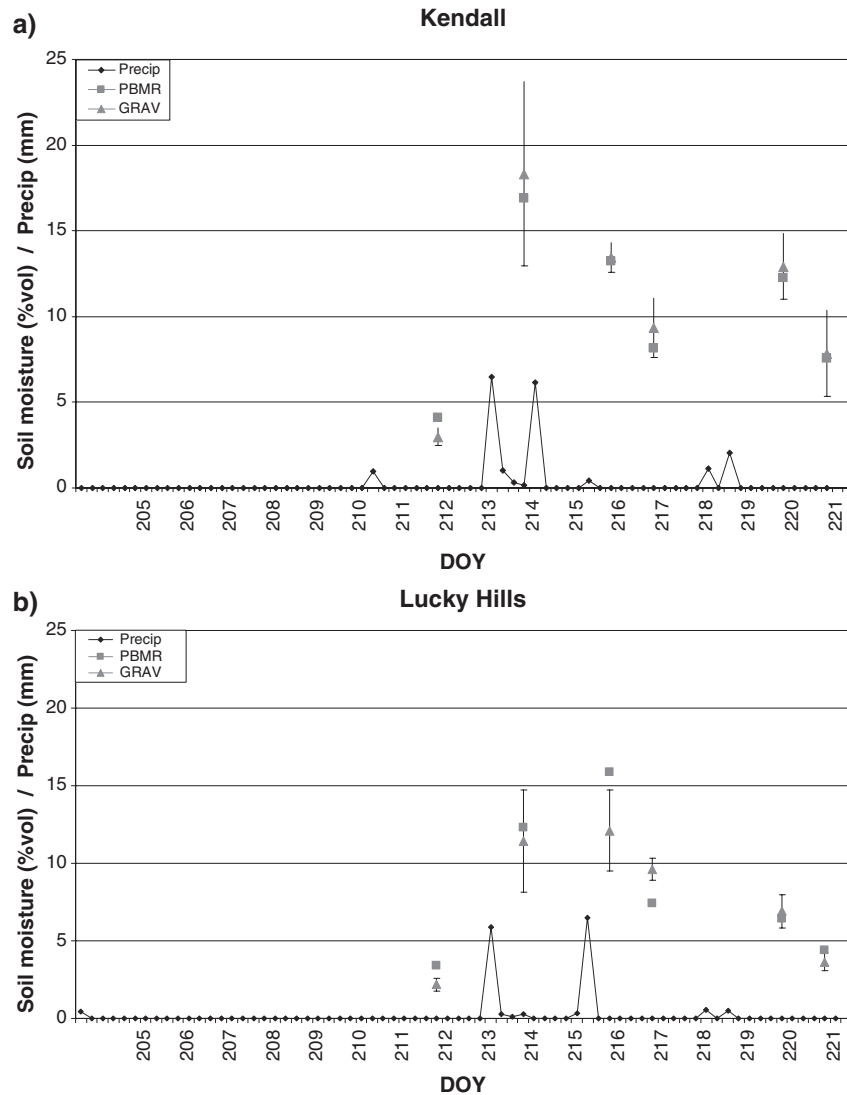


Fig. 2. Soil moisture in the 0–5 cm layer at the a) Kendall and b) Lucky Hills sites during the Monsoon '90 study period from (■) PBMR retrievals (Schmugge et al., 1994) and (▲) gravimetric measurements with standard deviations of the 3 measurements made at each site. Also plotted are the 6-hourly precipitation totals during the period at each site as derived from the 84-gauge-interpolated dataset over WGEW (Garcia et al., submitted for publication).

(6 m), and surface pressure. As suggested by Houser et al. (1998), the impacts of using of a single forcing dataset applied to the entire watershed are minimal so long as spatially distributed precipitation is accounted for, which is the case here. Indeed, simulations were performed using the Kendall forcing data in place of LH, and resulted in changes in surface fluxes that were less than the instrument error. To ensure that the most detailed precipitation data was included, rainfall from 84 of the 98-gauge network was broken down and interpolated in time and space at 20-minute and 40-meter resolution. Garcia et al. (submitted for publication) provide a detailed description and evaluation of two methods of interpolating rain gauge data over the WGEW, and for the large number of gauges available here both the inverse distance weighting (IDW) and multi-quadric biharmonic (MQB) schemes work equally well for precipitation interpolation.

The hydrology within the Noah model is handled by a Richards' equation formulation governed by the Campbell (1974) functions. Traditionally, hydraulic parameters are derived

at each grid cell from lookup tables from Cosby et al. (1984) based on soil texture maps. Typical sources of soil texture data for the U. S. include the Food and Agricultural Organization of the United Nations (FAO; FAO-UNESCO 1981), State Soil Geographic Database (STATSGO; USDA 1994), and Soil Survey Geographic Database (SSURGO; USDA, 2006). Soil type data from SSURGO is the highest-resolution (county-level) available continuously over the WGEW, and is used here in our default Noah simulations.

In a similar manner, vegetation parameters for each grid cell are derived from land cover maps (using lookup tables). Peters-Lidard et al. (submitted for publication) performed a thorough evaluation of the impacts of varying inputs of land cover, soil type, and precipitation on soil moisture simulations. In this study, we use the best available land cover data (UMD; Hansen et al., 2000), climatologically-derived values of albedo and vegetation fraction, and MQB precipitation forcing as input to the Noah model.

A standard 4-layer soil profile was used in Noah with a top layer of 5 cm that matched the representative depth of in-situ and remote sensing soil moisture measurements. The sensitivity of Noah to varying numbers (up to 20) and depths of soil layers was examined in detail, and results showed that adding additional layers did not significantly alter or improve results for this semi-arid region. Also, after careful calibration with observed soil moisture values in the WGEW and the results of previous studies (Scott et al., 2000), the prescribed minimum value of soil moisture in Noah was lowered from 0.05 to 0.02 m³ m⁻³.

In an effort to ensure consistency and add flexibility within soil types and hydraulic parameters, continuous PTFs were incorporated into Noah to replace lookup tables for this study. Specifically, the PTFs derived by Cosby et al. (1984) require only percentages of sand and clay to derive the hydraulic parameters as follows,

$$\theta_s = 0.489 - 0.00126 * \text{SAND} \quad (2)$$

$$\psi_s = \frac{10.0 \exp[1.88 - 0.0131 * \text{SAND}]}{100.0} \quad (3)$$

$$K_s = \frac{0.0070556 * 10.0 \exp[-0.884 + 0.0153 * \text{SAND}]}{1000.0} \quad (4)$$

$$b = 2.91 + 0.159 * \text{CLAY} \quad (5)$$

where θ_s (m³ m⁻³), ψ_s (m), K_s (m s⁻¹), and b are functions of SAND and CLAY percentage (%), and independent of soil texture classes or averaging. Though based on the identical soil samples and data of the default Noah lookup tables, these PTFs ensure that a full range of soil parameter values based on soil composition is derived in a realistic and consistent manner.

3.5. Parameter estimation

The Parameter Estimation model (PEST; Doherty, 2004) is a widely-used tool for examining sensitivities and estimating parameters in models spanning a wide range of applications. In particular, the ability of PEST as a model-independent estimation technique to link with any type of LSM using flexible parameter, observation, and convergence criteria make it optimal for use in this study. Here, PEST was configured to run as a parent model to Noah (PEST-Noah), where it evaluates and minimizes an objective function based on the differences between simulated and observed soil moisture as follows:

$$\text{RMSE} = \left[\frac{1}{N_{\text{obs}}} \sum_{i=1}^{N_{\text{obs}}} (\theta_{i,\text{Noah}} - \theta_{i,\text{PBMR}})^2 \right]^{0.5} \quad (6)$$

where N_{obs} is the number of PBMR observations used in the calibration and $\theta_{i,\text{Noah}}$ and $\theta_{i,\text{PBMR}}$ are Noah simulated and PBMR observed 0–5 cm soil moisture at each observation time. Until the convergence criteria are met, PEST iterates and adjusts the PTF parameters (sand, silt, and clay percentages), evaluates if this decreases the model error, and adjusts the parameters

accordingly. Extensive testing of PEST-Noah has shown that there can be on the order of 2–20 iterations requiring up to 200 model runs in total before PEST converges in some cases, depending on how far the initial parameters are from their optimal values.

To ensure the accuracy and repeatability of PEST-Noah simulations, identical twin experiments were conducted. PEST-Noah was run at the Kendall and LH sites using Noah soil moisture output from control simulations of widely varying soil types as observations (in place of PBMR). In each case PEST-Noah returned the precise sand, silt, and clay values prescribed in the control case and gives confidence to running PEST-Noah for a variety of conditions over WGEW and that the results are unique.

4. Results

4.1. M90 calibration experiments

Simulations were performed during the M90 period from 23 July–9 August 1990 that encompasses the 6 PBMR overpasses. This period allows ample time for the model to equilibrate to the very dry initial conditions leading up to the first PBMR image (31 July), and before the onset of the monsoon and the first significant precipitation event of the season (2 August). The model was run using a 20-minute timestep, and output was generated every 6 h.

4.1.1. Metflux sites

PEST-Noah was run at each of the 8 Metflux sites using the closest 40 m PBMR pixel to each site on the 6 observation dates. Fig. 3 shows the simulated soil moisture at the Kendall and LH sites before (SSURGO soils) and after (PEST) calibration of sand, silt, and clay along with corresponding PBMR and in-situ gravimetric measurements. Despite the differences in magnitude and drydown patterns exhibited between the sites, PEST is able to fit the simulated soil moisture to the observations. Also evident is the significant improvement in simulations using calibrated soil properties compared with those from default lookup table (SSURGO) approach.

The RMSE and bias in simulated versus observed (PBMR) soil moisture for all 8 Metflux sites are shown in Fig. 4. The ARMS requirement of 5% (volumetric) accuracy in soil moisture prediction is easily satisfied at all the Metflux sites when using the PEST-Noah calibration, with overall RMSE and bias values less than 2%. In particular, the bias in the default Noah simulation using SSURGO soils has been greatly reduced using PEST to near zero for most locations. Examination of each individual site's improvement in simulated soil moisture (similar to that shown in Fig. 3) makes it clear that PEST-Noah primarily acts to reduce the bias by adjusting the overall magnitude and dynamic range (using soil texture) to match observations.

Given the accuracy of the calibrated soil moisture at each site, it is useful to assess the potential utility and accuracy of optimized soil textures as well. Fig. 5 shows a comparison of the optimized sand, silt, and clay percentages at each site versus

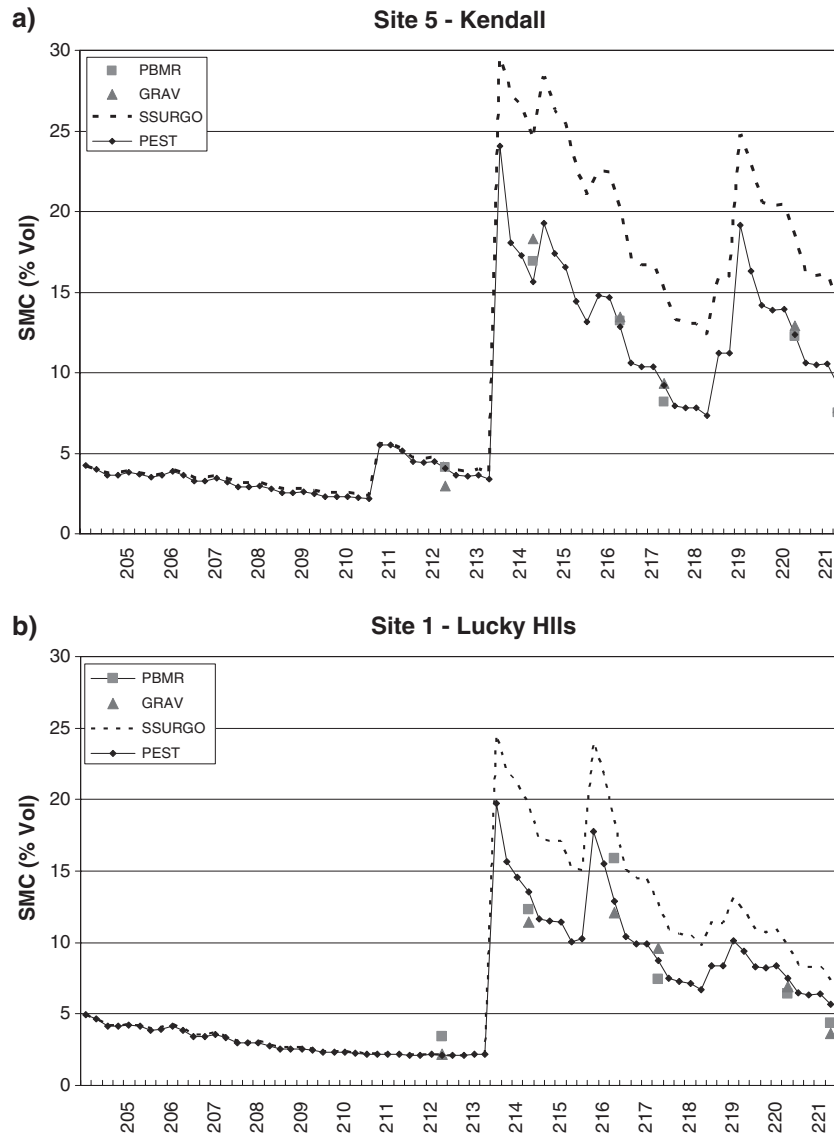


Fig. 3. Simulated 0–5 cm soil moisture from default and PEST-calibrated Noah simulations for the a) Kendall and b) Lucky Hills sites during the M90 period. Measurements of soil moisture from PBMR and gravimetric sensors on the 6 optimization dates are also shown.

those measured during the M90 experiment by [Schmugge et al. \(1994\)](#). The optimized soil textures suggest a primarily sandy soil, and are similar to the observed soils with greater than 65% sand and less than 10% clay content. Optimized values of silt content are lower than those observed, but this is likely due to the setup of PEST-Noah where silt is actually a dummy variable and, more importantly, that the PTFs are only a function of sand and clay content.

It is also important to consider the range and magnitude of hydraulic properties resulting from the different soil textures. [Table 1](#) presents the optimized values of sand, silt, and clay for the Metflux sites and corresponding hydraulic properties derived from the PTFs in Noah. For comparison, [Table 1b](#) lists observed soil textures from [Schmugge et al. \(1994\)](#) and hydraulic properties at each site estimated using the Noah PTFs. Overall, there is relatively little variation in properties estimated from PEST-Noah across the sites despite variation in sand content (73–100%). Similarly, hydraulic properties derived

from observed textures exhibit a small range, although their magnitude differs slightly from the PEST-Noah values due to the lower sand percentage (66–80%).

To get a better feel for the physical applicability of the parameters themselves, [Table 2](#) presents hydraulic parameters derived from FAO, STATSGO, and SSURGO soil lookup tables, a neural network-based PTF (ROSETTA; [Schaap et al., 1998](#)), PEST-Noah using PTFs, and measurements made during 2002 ([Schaap & Shouse, 2004](#)) and the 2004 North American Monsoon Experiment (NAME; [Higgins et al., 2006](#)). The FAO soil type for all 8 Metflux sites is sandy loam, STATSGO is loamy sand, and the finer resolution SSURGO data indicates 3 different soil types across the Metflux sites. As a result, there is significant disagreement in hydraulic properties among these lookup tables alone.

The PEST-Noah parameters fall within the range of established datasets and measurements, yet there remain significant differences between lookup table and calibrated hydraulic

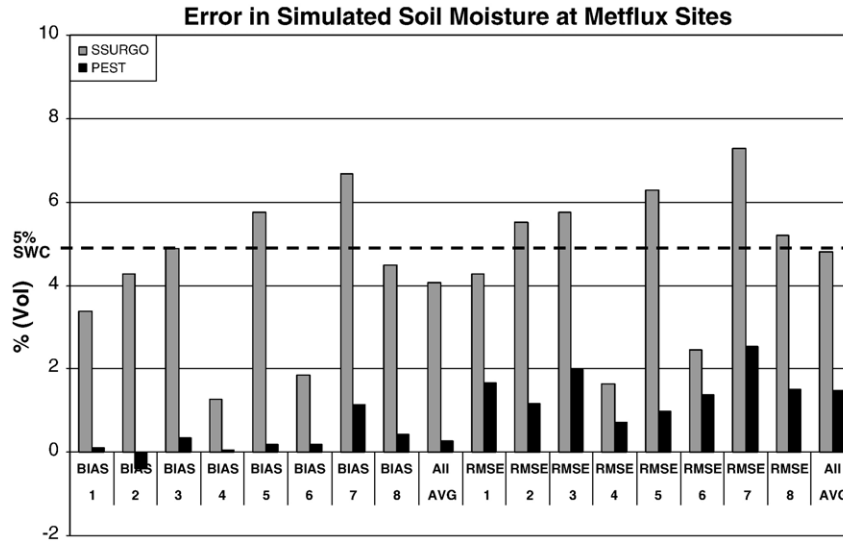


Fig. 4. Bias and RMSE in simulated versus observed (PBMR) 0–5 cm soil moisture during the M90 period using default (SSURGO; gray) and optimized (PEST; black) soil properties at each Metflux site.

properties as a result of using continuous PTFs in PEST-Noah. The ROSETTA PTF model suggests parameters that are inconsistent for a sandy soil and with observations, and indicate this particular PTF may not be appropriate for this region. Based on the improvements in simulated soil moisture exhibited by PEST-Noah presented earlier, the PEST-Noah soil textures and PTFs appear to be the most accurate.

From a broader perspective, it is important to assess whether PEST-derived soil parameters can be employed in Noah and represent conditions at WGEW over longer timescales. Therefore, the soil textures optimized from the M90 period were used to run the Noah model at Kendall and LH over the 2002–4 evaluation period. Fig. 6 shows the soil moisture simulated by Noah over a 54-day period (following an 18 month spinup) in the summer of 2003 compared with in-situ observations from Vitel

probes surrounding LH and Kendall. Simulations with optimized parameters (RMSE=2.8/2.9, Bias=-0.01/-0.02% volumetric for LH and Kendall, respectively) perform well and are comparable to those using SSURGO soils (RMSE=4.2/3.6, Bias=2.4/.01%) over the extended period. Once again, this highlights the ability of PEST to adjust the dynamic range of soil moisture simulated by Noah and effectively respond to precipitation events, and supports the use of optimized soil properties across this watershed for seasonal (and longer) durations that are equal or better than high-resolution soil maps.

4.1.2. Watershed average

As detailed point or regional surface characteristics are not always available, it is useful to examine the calibration technique at lower spatial resolution. Fig. 7 shows simulated soil

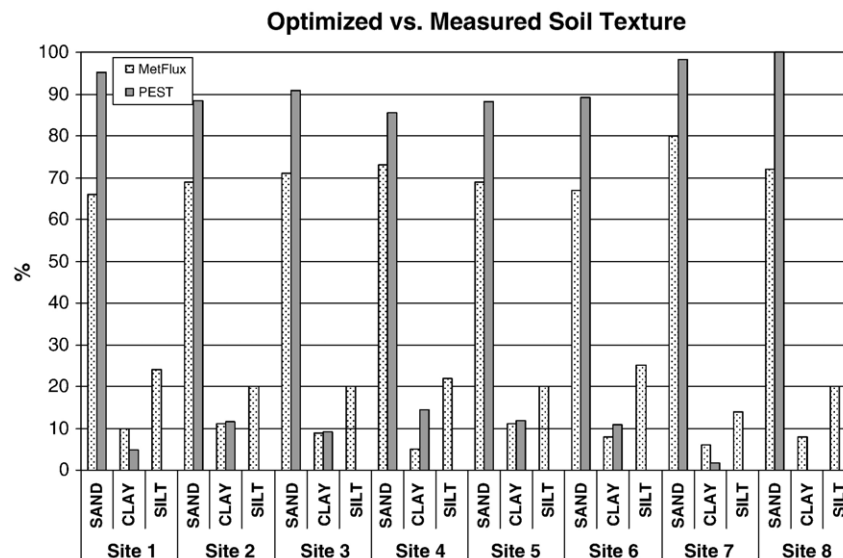


Fig. 5. Percentages of sand, silt, and clay estimated by PEST-Noah at the eight Metflux sites compared with in-situ measurements from Schumgege et al. (1994).

Table 1
Optimized sand, silt, and clay percentages estimated from a) PEST-Noah simulations at the eight Metflux sites compared with b) those observed by Schmutge et al. (1994) and associated hydraulic properties computed for each using the PTFs employed in the Noah LSM (Cosby et al., 1984)

a)								
PEST Site	% SAND	% SILT	% CLAY	K_{sat} (m s ⁻¹)	K_{sat} (cm d ⁻¹)	'b'	θ_s (m ³ m ⁻³)	ψ_{sat} (m)
1 (LH)	95.3	0.0	4.7	2.65 E-05	228.6	3.66	0.369	0.043
2	88.5	0.0	11.5	2.08 E-05	179.9	4.74	0.377	0.053
3	90.9	0.0	9.1	2.27 E-05	195.8	4.36	0.374	0.049
4	85.5	0.0	14.5	1.87 E-05	161.9	5.22	0.381	0.057
5 (Kendall)	88.3	0.0	11.7	2.07 E-05	178.7	4.77	0.378	0.053
6	89.1	0.0	10.9	2.13 E-05	183.8	4.64	0.377	0.052
7	98.3	0.0	1.7	2.94 E-05	254.1	3.18	0.365	0.039
8	100.0	0.0	0.0	3.12 E-05	269.8	2.91	0.363	0.037
b)								
Observed Site	% SAND	% SILT	% CLAY	K_{sat} (m s ⁻¹)	K_{sat} (cm d ⁻¹)	'b'	θ_s (m ³ m ⁻³)	ψ_{sat} (m)
1	66	24	10	9.42 E-06	81.4	4.5	0.406	0.104
2	69	20	11	1.05 E-05	90.7	4.7	0.402	0.095
3	71	20	9	1.12 E-05	96.8	4.3	0.399	0.089
4	73	22	5	1.21 E-05	104.5	3.7	0.397	0.084
5	69	20	11	1.05 E-05	90.7	4.7	0.402	0.095
6	67	25	8	9.76 E-06	84.3	4.2	0.405	0.101
7	80	14	6	1.54 E-05	133.1	3.9	0.388	0.068
8	72	20	8	1.16 E-05	100.2	4.2	0.398	0.086

moisture across the entire PBMR domain on DOY 214 from default (SSURGO) Noah and PEST-Noah simulations compared with the PBMR data. In this case, PEST-Noah is minimizing the *mean* error in simulated versus observed soil moisture across this watershed. DOY 214 was chosen because it is just after the onset of precipitation when the hydraulic

parameters have the largest impact on soil moisture. While there is only one set of optimized soil texture and hydraulic parameters estimated for the entire domain (92% sand, 8% clay), the significant improvement (RMSE and bias) in PEST-Noah soil moisture over that simulated using SSURGO data indicates that the calibration process can still be successful and potentially

Table 2
Soil hydraulic parameters used in the Noah model at the a) Kendall and b) Lucky Hills sites derived from default lookup tables based on FAO, STATSGO, and SSURGO classifications and those computed from PEST-Noah estimates of sand, silt, and clay percentages at each site using the PTFs in Noah

a)							
Kendall	FAO	STATSGO	SSURGO	ROSETTA	PEST	NAME	2002
Soil type	Sandy loam	Loamy sand	Clay loam	Sandy loam	Loamy sand	Sandy loam	Sa. clay loam
K_{sat} (m s ⁻¹)	5.2 E-05	1.41 E-05	2.5 E-05	2.9 E-05	2.07 E-05	1.4–4.2 E-05	1.04 E-05
K_{sat} (cm d ⁻¹)	44.3	121.8	21.6	24.9	178.66	120.9–362.9	898.6
'b'	4.74	4.26	8.17	–	4.77	–	1.96
θ_s (m ³ m ⁻³)	0.43	0.42	0.47	0.25	0.378	0.33	0.47
ψ_{sat} (m)	0.14	0.04	0.26	–	.053	–	0.21
θ_{ref} (m ³ m ⁻³)	0.28	0.26	0.29	–	0.22	–	–
θ_{wilt} (m ³ m ⁻³)	0.047	0.029	0.103	0.031	.020	–	–
b)							
Lucky Hills	FAO	STATSGO	SSURGO	ROSETTA	PEST	NAME	2002
Soil type	Sandy loam	Loamy sand	Sa. clay loam	Sandy loam	Sand	Sand	Sa. clay loam
K_{sat} (m s ⁻¹)	5.2 E-05	1.41 E-05	4.5 E-05	2.5 E-05	2.65 E-05	1.4–4.2 E-05	1.65 E-05
K_{sat} (cm d ⁻¹)	44.3	121.8	38.9	21.2	228.63	120.9–362.9	1425.6
'b'	4.74	4.26	6.77	–	3.66	–	1.62
θ_s (m ³ m ⁻³)	0.43	0.42	0.40	0.24	0.369	0.25	0.45
ψ_{sat} (m)	0.14	0.04	0.14	–	.043	–	0.16
θ_{ref} (m ³ m ⁻³)	0.28	0.26	0.26	–	0.18	–	–
θ_{wilt} (m ³ m ⁻³)	0.047	0.029	0.069	0.028	.020	–	–

For comparison, soil properties estimated by Scott et al. (2000) from a neural network PTF (ROSETTA; Schaap et al., 1998) are shown along with site-specific estimates of hydraulic parameters based on soil samples taken during 2002 (Schaap & Shouse, 2004) and during the NAME (Higgins et al., 2006) in 2004.

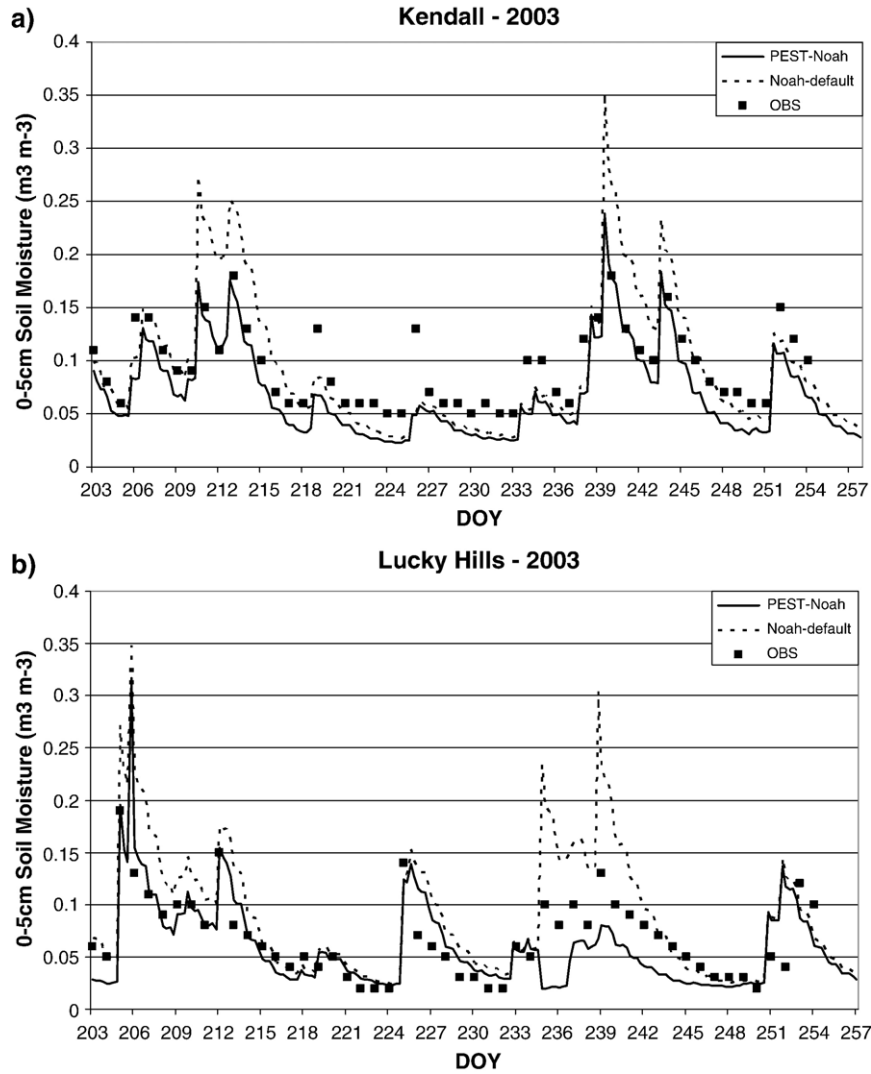


Fig. 6. Near-surface soil moisture simulated by Noah using PEST-derived soil properties and default soil parameters (SSURGO) compared against Vitel probe observations at the a) Kendall and b) Lucky Hills sites during summer 2003.

useful for deriving meaningful soils data on watershed scales with coarser inputs.

4.2. Temporal sampling of PBMR images

The high temporal resolution of the PBMR imagery captures a complete soil drying cycle for this region. To assess the broader applicability of the methodology described above, it is useful to look at precisely how many and which PBMR images are needed for accurate calibration. The sensitivity of PEST-Noah to the number of PBMR observations was tested by looking at all possible combinations of image in the calibration process. Fig. 8a shows the error in simulated versus observed soil moisture at Kendall for each of the image combinations used in PEST-Noah. Kendall was chosen as a representative site because it exhibits the largest range of soil moisture throughout the period and also was more difficult to calibrate due to two significant precipitation events and a strong drydown period in between.

Fig. 8a shows that there is a significant reduction in RMSE (and standard deviation) once three or more images are used in the calibration. There are fewer number of data points for single images because many of those simulations were unable to converge with only one observation. What is also evident is a large amount of scatter or variability when using one or two images, while for simulations employing three or more observations all the points collapse indicating that it does not matter which images are included. Note that the error using Noah with SSURGO soils (Fig. 4) is still 2–3 times larger than even the worst PEST-Noah simulations using a single PBMR image.

The other main factor in the success of PEST-Noah is what portion of the soil drying curve (i.e. dynamic range) is captured by the PBMR images. Fig. 8b shows the error in simulated soil moisture against the range in soil moisture captured by the image combinations described above. The results look similar to Fig. 8a, and suggest that errors are significantly reduced if the images used capture at least 5% (volumetric) variability in soil moisture during a drydown period. When the full dynamic

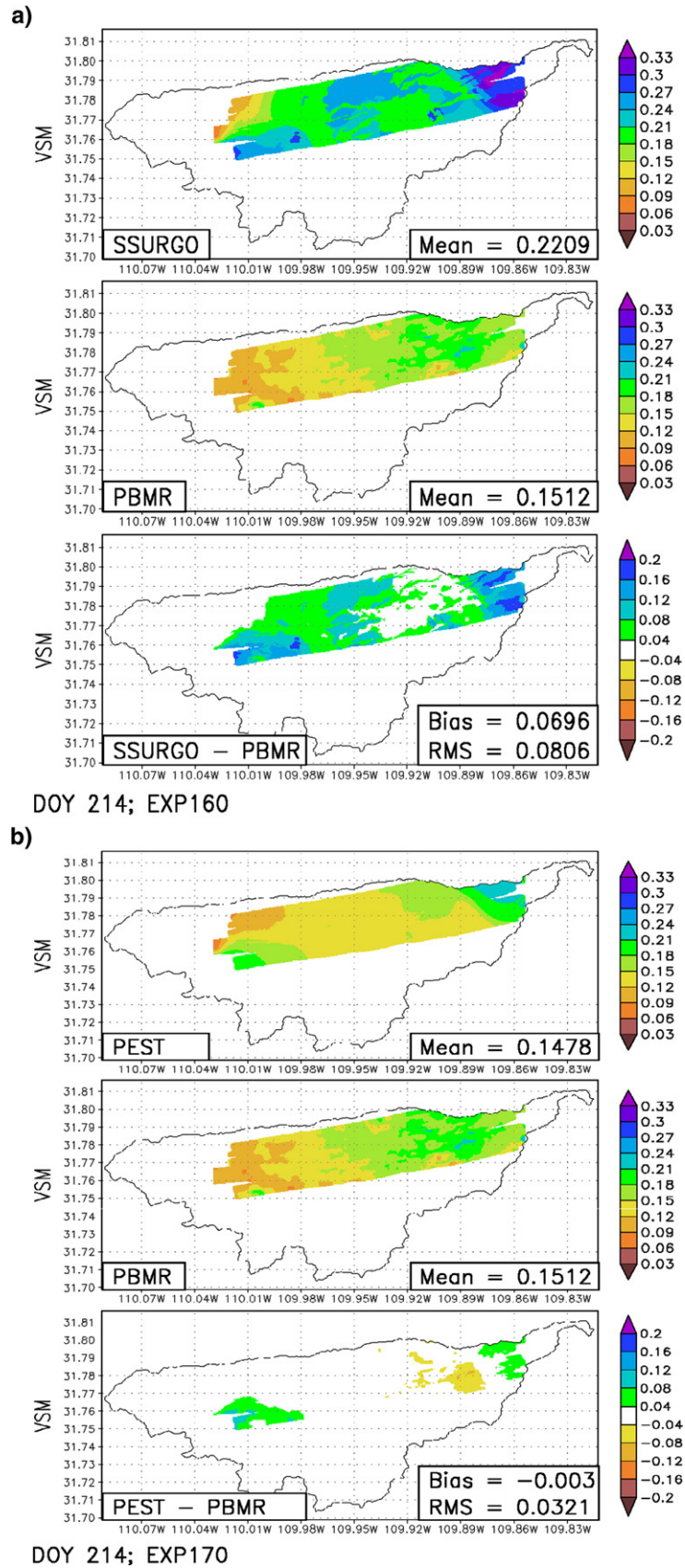


Fig. 7. RMSE and bias in simulated versus observed 0–5 cm soil moisture using a) default (SSURGO) soils and b) soil properties optimized using PEST-Noah on DOY 221. A single set of parameters was optimized for the entire PBMR domain.

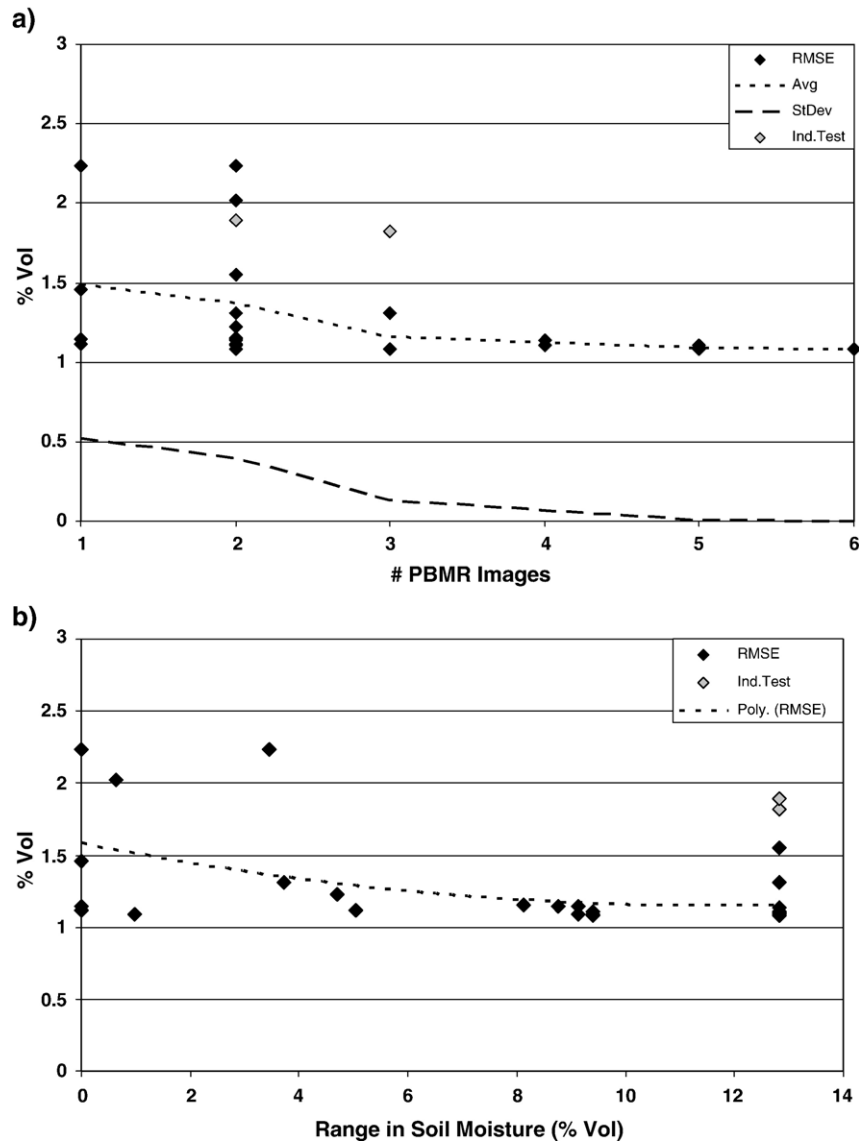


Fig. 8. Errors in simulated versus observed 0–5 cm soil moisture at the Kendall site for varying a) numbers of PBMR images used in PEST-Noah and b) ranges of soil moisture covered by these images. The lightly shaded points indicate simulations that were calibrated using only the first two and three PBMR images.

range in soil moisture is captured by the PBMR images, the RMSE and bias (not shown) in PEST-Noah simulations are minimized, and are ~5 times lower than using SSURGO soils.

Analyses also indicate that the second PBMR image (DOY 214) is the most critical observation to include in the calibration. This image was acquired immediately following a rainfall event (Fig. 2a) and represents the maximum value of soil moisture observed during the period. Out of the 7 simulations when PEST-Noah was unable to converge on a solution (i.e. not enough information was coming from the observations), all occurred when day 214 was not included. More importantly, out of the simulations using 5 out of 6 images, the only one unable to converge was with day 214 omitted. Error analyses (not shown) also support the importance of including day 214, and the improvement in calibrations when this ‘wet’ image is included.

An independent test of the sensitivity of PEST-Noah to the choice of PBMR images was also conducted, using only the

first 2 and 3 PBMR images to calibrate the model and evaluating Noah with the optimized soils over the remainder of the period. The errors in simulated soil moisture using this approach are also plotted in Fig. 8, and similar to those timescales, PEST-Noah could be used with a few images early in the period to calibrate and estimate soil properties, which could then be used to improve simulations on a forecast basis without requiring additional images.

4.3. 2003 Calibration experiments

The development of the delta index allows us to test the PEST-Noah approach using satellite-based active radar imagery. RADARSAT-1 images were acquired over the WGEW during July, August, and September 2003 that cover a larger temporal and spatial extent than the PBMR images during the M90 period (Fig. 9). As described earlier, the Delta Index data had to be aggregated from 40 to 210 and 280 m resolution to reduce the

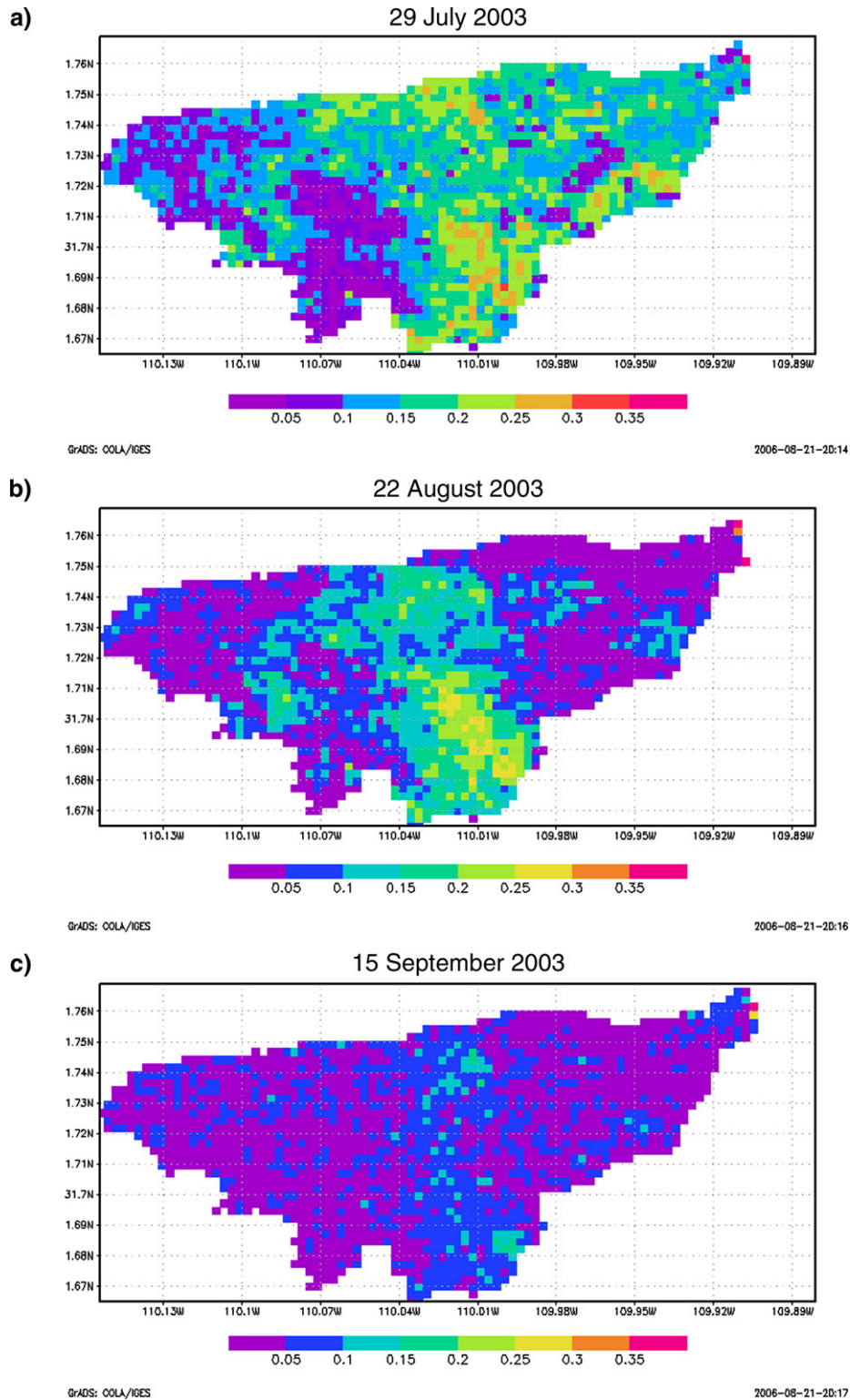


Fig. 9. Soil moisture ($\text{m}^3 \text{m}^{-3}$) estimated from RADARSAT-1 active microwave measurements over the WGEW on a) 29 July, b) 22 August, and c) 15 September 2003. Backscatter was aggregated from 7 to 280 m to reduce the effects of speckle and converted to soil moisture using the delta index image differencing technique (Thoma et al., 2006).

impact of speckle (amplified by the high rock content of the soils in this region) on the soil moisture retrievals. Although PEST-Noah was run with precipitation and land cover data at 40 m resolution, experiments were conducted to confirm the

appropriateness of applying 210 and 280 m resolution data from active radar to that of a 40 m pixel.

To cover the extended period between radar overpasses, PEST-Noah was run from 30 June–15 September 2003 using

the interpolated precipitation and Kendall forcing data as for the 2003 evaluations described previously. Fig. 10a shows the PEST-Noah simulations, delta index estimates, and in-situ observations of soil moisture at the Kendall site. Once again, PEST-Noah does a good job of calibrating the parameters in Noah to produce soil moistures that match those estimated by the delta index. For the Kendall site, PEST-Noah converged on a solution of 100% sandy soil for both the 210 and 280 m images (compared with 88% sand; 12% clay in M90). Although this calibration suggests a slightly sandier soil than M90, the differences in soil moisture and hydraulic properties are negligible, as discussed in Section 4a. The higher sand content is likely the result of the slightly lower mean range of soil moisture estimated by the delta index (0.153 max, 0.032 min) as compared to the PBMR (0.169 max, 0.075 min), which requires a soil type that drains more readily.

The PEST-Noah results for LH (Fig. 10b) suggest considerable differences in calibrations using the delta index compared with observations and PBMR calibrations. The optimized values for sand, clay, and silt were 28, 72, and 0% using 210 m data, and

20, 45, and 35% using 280 m data (compared with 95% sand; 5% clay in M90). Closer inspection of the in-situ observations of soil moisture over the period shows a comparable dynamic range to that observed at Kendall. However, the first delta index image (at both 210 and 280 m) gives a rather wet soil moisture estimate compared to observations, while the latter 2 images are relatively dry. In order to match the high moisture content of the first image, PEST-Noah is forced to simulate a high clay content which has a higher holding capacity and strength.

The first radar overpass is nearly 3 days after the last significant rainfall at LH, which means the soil has had significant time to dry out particularly for this region. In fact, studies have shown that the typical response time from rainfall to complete drydown is within 2–3 days (or less, depending on ground cover) in WGEW due to the shallow moisture reservoir and high bare soil evaporation rates (Kurc & Small, 2004; Shamir et al., 2005). That previous studies, M90 observations (PBMR and in-situ), and in-situ observations all depict a much more rapidly drying soil at the site suggests that the delta index data may be overestimating soil moisture on this date.

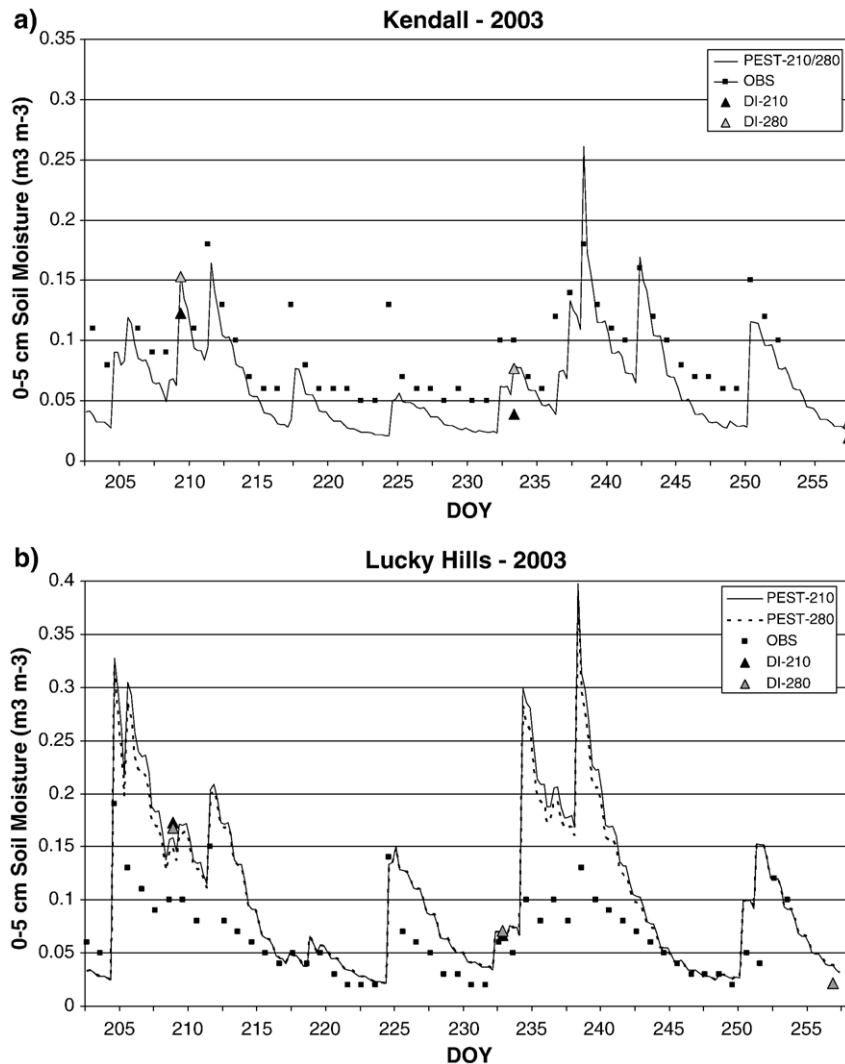


Fig. 10. Near-surface soil moisture simulated by PEST-Noah using 210 and 280 m Delta Index as observations at the a) Kendall and b) Lucky Hills sites during summer 2003. Also shown are observations of soil moisture from Vitel probes surrounding each location.

5. Discussion

While PEST-Noah suggests a slightly more sandy soil over the region than observed during M90, the differences in the parameters that control the soil moisture dynamics are not as significant as the soil textures might indicate. Plausible values are estimated by PEST-Noah for each parameter when compared with established datasets and measurements (Tables 1 and 2). This is due to the slowly varying relationships between soil texture and hydraulic properties for high sand contents governed by the PTFs.

Further, it has been noted in numerous studies of the WGEW that there is an unusually high rock fragment content of the upper soil layers (and is not typically accounted for in categorical lookup tables or PTFs). The unique and sandy soil type estimated by PEST-Noah at the Metflux sites is slightly less porous and more conductive than those observed, which may be an attempt to indirectly account for the high rock content in Noah by adjusting the parameters to match that of a rocky, yet sandy, soil (i.e. less pore space but increasing flow paths in the soil volume). A simple formulation to account for rock content in calculating hydraulic parameters is currently being implemented in the Noah model to test the sensitivity of the calibrations.

There remain significant differences between lookup table and calibrated hydraulic properties. This is due to the ability of the continuous PTFs implemented PEST-Noah to produce in a unique (but realistic) soil type that rigid lookup tables cannot describe. It is also important to note that the large spread of hydraulic properties across data sources in Table 2 is a function of differences in the way each property is estimated and what each represents. For example, K_{sat} values of 250 cm d^{-1} can be estimated from soil samples under laboratory conditions, even though actual precipitation rates could never be high enough to observe similar saturation values in the field. Further, while the ROSETTA model suggests values for K_{sat} that are an order of magnitude lower than those calculated in the laboratory (and may be closer to a true saturated value observed in nature), such values result in inaccurate simulations of soil moisture when employed in Noah. Overall, it is the combination of an accurate soil hydraulic property representation with the physics of the LSM that determines the most appropriate parameters.

Because PEST-Noah suggests a unique soil type that also corresponds well with observations, the limitations of the Noah soil physics do not appear to be significant enough to deter estimates of physically meaningful soil properties. On the contrary, attempts at calibrating more sophisticated vadose zone models have typically yielded parameter values that lie well outside measured values, and as such could only be interpreted as ‘effective values’ that absorb significantly more model or forcing data deficiencies than they do represent real soil properties. For example, Scott et al. (2000) found values of 2.5×10^{-6} and $3.7 \times 10^{-7} \text{ m s}^{-1}$ for K_{sat} and 0.25 and 0.23 $\text{m}^3 \text{ m}^{-3}$ for porosity at Kendall and LH, using a model calibration approach. Using the PTFs, these K_{sat} values correspond to a soil texture of 39% sand, and the porosity values are so low that a soil type cannot be derived. In contrast, the methodology presented in this paper

allows for calibrated parameters to be constrained by physical plausibility and the PTF approach, which, while subject to error, at least forces physical consistency.

With regards to the delta index experiments, which represent the first attempt to calibrate soil properties using satellite-based soil moisture estimates, high frequency (active) microwave retrievals are difficult to obtain in regions with high rock content due to increased backscatter and a weaker relationship with soil moisture (Jackson, 1992). Clearly, if there were more images available during 6-week period, particularly during and immediately following rainfall events, PEST-Noah would be able to perform better as for the M90 case. Houser et al. (1998) made similar recommendations for data assimilation in this region, suggesting that soil moisture observations are required at least once during every storm event. For the 2003 experiments, it is likely a combination of insufficient temporal sampling and the limited spatial resolution of active remote sensing (through the signal-to-noise ratio) in the soil moisture retrieval process that resulted in poor calibration at LH.

Along these lines, the resolution of the precipitation data is a critical factor for the calibration process. While the results here present a ‘best-case’ scenario in terms of the spatial and temporal resolution of (84-gauge) rainfall data, it is important to consider the applicability of these results to semi-operational applications in regions of limited precipitation observations. To address this, a companion study has been conducted (Peters-Lidard et al., submitted for publication) which demonstrates the sensitivity of the calibration and soil property retrieval process to a range of precipitation resolutions for the identical watershed and time period presented in this paper.

6. Conclusions

This paper has examined a straightforward method of using microwave remote sensing of near-surface soil moisture to calibrate an offline land surface model, and in the process infer soil texture and hydraulic properties at high spatial resolutions. This approach expands and improves upon a wide body of previous work by incorporating pedotransfer functions into the LSM to ensure consistent and physically meaningful soil parameters, and by addressing the temporal sampling of remote sensing imagery needed for successful calibration. As a testbed for the ARMS project, this research was able to retrieve soil texture and property estimates that correspond well with observed soils over the WGEW. Once estimated for this region, these parameters were also used to simulate soil moisture over seasonal time scales with a great deal of accuracy compared to simulations with default soils and soil properties based on lookup tables.

Specific results of this study include the following:

- 1) Limited microwave retrievals of near-surface soil moisture can be used to calibrate an LSM to within .02 $\text{m}^3 \text{ m}^{-3}$ accuracy at high temporal and spatial resolutions.
- 2) Optimizing soil hydraulic properties using PTFs gives better and more physically meaningful results than a one-at-a-time parameter estimation approach.

- 3) Errors in the calibration process are minimized when there are at least 3 images included that represent the typical range of moisture exhibited by the soil type during a drydown period.
- 4) Independent tests indicate that this methodology can be successful in calibrating LSMs over seasonal and longer timescales for use in specialized prediction systems.

Overall, these results suggest that ARMS could be applied at sparsely-vegetated locations to simulate soil moisture in a semi-operational context with limited remote sensing inputs. Simulations that expand the 8 Metflux sites tested here to the full WGEW at 40 m resolution of PEST-Noah are ongoing, from which fully distributed maps of soil texture and hydraulic properties will be produced. Alternatively, one could use the PEST-Noah approach after stratifying the watershed using high-resolution soils, land cover, or similar data to further examine the spatial distribution of soil properties. Distributed soil property information can then be compared with existing soils maps and the approach repeated and applied to other LSMs and regions. Future work on the ARMS project will include testing the methodology and evaluating the delta index at cold land, high relief, and strongly coupled (land–atmosphere) regions of the U. S., where the calibration process should yield new insight on the images and accuracy required and the limitations of LSM physics for diverse surface conditions.

The ability of satellite-based active remote sensing and the delta index technique to retrieve soil moisture on scales smaller than watershed needs to be investigated further before incorporation in an ARMS type of approach. While results here have shown that 3 images are sufficient to calibrate and obtain soils information, the soil moisture estimates must be accurate (within ~3–5%) and capture a typical dynamic range of soil moisture for the region in question. Currently, vegetation cover is another limiting factor for both L-band and C-band retrievals of near-surface soil moisture, and as a consequence, the ARMS approach.

The spatial resolution of currently orbiting active remote sensing, determined in part by the signal-to-noise ratio of the measurement, may be a limiting issue for this application. As such, the accuracy of soil moisture retrieval from active remote sensing through approaches like the delta index or other retrieval methods (e.g. Alvarez-Mozos et al., 2005) needs further investigation before it can be incorporated with confidence. With this in mind, the ARMS methodology should be considered using platforms other than those considered here. For example, current microwave sensors aboard satellites provide limited soil moisture information at regional scales (generally 6–20 GHz, 38–70 km horizontal resolution), and the future Soil Moisture and Ocean Salinity (SMOS; Pellarin et al., 2003) mission will be the first to provide L-band retrievals on a global scale (1.4 GHz, 50 km).

Acknowledgments

This work was supported by the Army Remote Moisture System project under Reimbursable Agreement Number 60-

5342-3-0363 between USDA/ARS and NASA-GSFC. We would like to thank the Tombstone and ARS-SWRC staff for their data and site information support. Special thanks are extended to Dr. Thomas Schmutge for insight into the PBMR retrievals, Dr. Paul Houser for use of some WGEW input fields and datasets, and Dr. Sujay Kumar for help with the PEST-Noah integration. We also greatly appreciate the personal communication and assistance of John Doherty with the implementation of PEST.

References

- Ahuja, L. R., Wendroth, O., & Nielsen, D. R. (1993). Relationship between initial drainage of surface soil and average profile saturated conductivity. *Soil Science Society of America Journal*, 57, 19–25.
- Alvarez-Mozos, J., Casali, J., Gonzalez-Audicana, M., & Verhoest, N. E. C. (2005). Correlation between ground measured soil moisture and RADAR-SAT-1 derived backscattering coefficient over an agricultural catchment of Navarre (north of Spain). *Biosystems Engineering*, 92, 119–133.
- Berberly, E. H., Luo, Y., Mitchell, K. E., & Betts, A. K. (2003). Eta model estimated land surface processes and the hydrologic cycle of the Mississippi basin. *Journal of Geophysical Research*, 108, 8852.
- Betts, A. K. (2000). Idealized model for equilibrium boundary layer over land. *Journal of Hydrometeorology*, 1, 507–523.
- Betts, A. K., Ball, J. H., Bosilovich, M., Viterbo, P., Zhang, Y., & Rossow, W. B. (2003). Intercomparison of water and energy budgets for five Mississippi subbasins between ECMWF reanalysis (ERA-40) and NASA Data Assimilation Office fvGCM for 1990–1999. *Journal of Geophysical Research*, 108, 8618.
- Braun, F. J., & Schadler, G. (2005). Comparison of soil hydraulic parameterizations for mesoscale meteorological models. *Journal of Applied Meteorology*, 44, 1116.
- Brooks, R. H., & Corey, A. T. (1964). Hydraulic properties of porous media. *Hydrol. Pap., Vol. 3*. Fort Collins: Colorado State Univ.
- Burke, E. J., Gurney, R. J., Simmonds, L. P., & Jackson, T. J. (1997). Calibrating a soil water and energy budget model with remotely sensed data to obtain quantitative information about the soil. *Water Resources Research*, 33, 1689–1697.
- Burke, E. J., Gurney, R. J., Simmonds, L. P., & O'Neill, P. E. (1998). Using a modeling approach to predict soil hydraulic properties from passive microwave measurements. *IEEE Transactions on Geoscience and Remote Sensing*, 36, 454–462.
- Camillo, P. J., O'Neill, P. E., & Gurney, R. J. (1986). Estimating soil hydraulic parameters using passive microwave data. *IEEE Transactions on Geoscience and Remote Sensing*, GE-24, 930–936.
- Campbell, G. S. (1974). A simple method for determining unsaturated conductivity from moisture retention data. *Soil Science*, 117, 311–314.
- Carlson, T. N., Gillies, R. R., & Schmugge, T. J. (1995). An interpretation of methodologies for indirect measurement of soil water content. *Agricultural and Forest Meteorology*, 77, 191–205.
- Chen, F., Mitchell, K., Schaake, J., Xue, Y., Pan, H., Koren, V., et al. (1996). Modeling of land-surface evaporation by four schemes and comparison with FIFE observations. *Journal of Geophysical Research*, 101, 7251–7268.
- Cosby, B. J., Hornberger, G. M., Clapp, R. B., & Ginn, T. R. (1984). A statistical exploration of the relationships of soil moisture characteristics to the physical properties of soils. *Water Resources Research*, 20, 682–690.
- Cuenca, R. H., Ek, M., & Mahrt, L. (1996). Impact of soil water property parameterization on atmospheric boundary layer simulation. *Journal of Geophysical Research Atmosphere*, 101, 7269–7277.
- Doherty, J. (2004). *PEST: Model independent parameter estimation. Fifth edition of user manual*. Brisbane, Australia: Watermark Numerical Computing.
- Ek, M., & Cuenca, R. H. (1994). Variation in soil parameters: Implications for modeling surface fluxes and atmospheric boundary-layer development. *Boundary - Layer Meteorology*, 70, 369–383.
- Ek, M. B., & Holtslag, A. A. M. (2003). Influence of soil moisture on boundary layer cloud development. *Journal of Hydrometeorology*, 5, 86–99.

- Ek, M. B., Mitchell, K. E., Lin, Y., Rogers, E., Grunmann, P., Koren, V., et al. (2003). Implementation of Noah land surface model advances in the National Centers for Environmental Prediction operational mesoscale Eta model. *Journal of Geophysical Research*, 108(D22), 8851.
- Entekhabi, D., Ghassem, R., Asrar, R., Betts, A. K., Beven, K. J., Bras, R. L., et al. (1999). An agenda for land surface hydrology research and a call for the second international hydrological decade. *Bulletin of the American Meteorological Society*, 79, 2743–2746.
- FAO-UNESCO (1981). *Soil map of the world, ten volumes, food and agriculture organization, Rome*.
- Feddes, R. A., Menenti, M., Kabat, P., & Bastiaanssen, W. G. M. (1993). Is large-scale inverse modelling of unsaturated flow with a real average evaporation and surface soil moisture as estimated from remote sensing feasible? *Journal of Hydrology*, 143, 125–152.
- Findell, K. L., & Eltahir, E. A. B. (2003). Atmospheric controls on soil moisture-boundary layer interactions. Part I: Framework development and part II: Feedbacks within the continental United States. *Journal of Hydrometeorology*, 4, 552–583.
- Garcia, M., Peters-Lidard, C. D. & Goodrich, D. C. (submitted for publication). Spatial interpolation of precipitation in a dense gauge network for monsoon storm events in the southwestern U.S. *Water Resources Research*.
- Gupta, H. V., Bastidas, L. A., Sorooshian, S., Shuttleworth, W. J., & Yang, Z. L. (1999). Parameter estimation of a land surface scheme using multi-criteria methods. *Journal of Geophysical Research*, 104, 19,491–19,504.
- Gutmann, E. D., & Small, E. E. (2005). The effect of soil hydraulic properties vs. soil texture in land surface models. *Geophysical Research Letters*, 32, L02402.
- Hansen, M. C., Defries, R. S., Townshend, J. R. G., & Sohlberg, R. (2000). Global land cover classification at 1 km spatial resolution using a classification tree approach. *International Journal of Remote Sensing*, 21, 1331–1364.
- Hess, R. (2001). Assimilation of screen-level observations by variational soil moisture analyses. *Meteorology and Atmospheric Physics*, 77, 145–154.
- Higgins, W., Ahijevych, D., Amador, J., Barros, A., Berbery, E. H., Caetano, E., et al. (2006). The NAME 2004 field campaign and modelling strategy. *Bulletin of the American Meteorological Society*, 87, 79–94.
- Hogue, T. S., Bastidas, L., Gupta, H., Sorooshian, S., Mitchell, K., & Emmerich, W. (2005). Evaluation and transferability of the Noah land surface model in semiarid environments. *Journal of Hydrometeorology*, 6, 68–84.
- Hollenbeck, K. J., Schumge, T. J., Hornberger, G. M., & Wang, J. R. (1996). Identifying soil hydraulic heterogeneity by detection of relative change in passive microwave remote sensing observations. *Water Resources Research*, 32, 139–148.
- Houser, P. R., Shuttleworth, W. J., Famiglietti, J. S., Gupta, H. V., Syed, K. H., & Goodrich, D. C. (1998). Integration of soil moisture remote sensing and hydrologic modeling using data assimilation. *Water Resources Research*, 34, 3405–3420.
- Jacobs, C. M. J., & Debruin, H. A. R. (1992). The sensitivity of regional transpiration to land-surface characteristics — Significance of feedback. *Journal of Climate*, 5, 683–698.
- Jackson, T. J. (1992). Rock fraction effects on the interpretation of microwave emission from soils. *IEEE Transactions on Geoscience and Remote Sensing*, 30, 610–616.
- Koster, R. D., Dirmeyer, P. A., Guo, Z., Bonan, G., Chan, E., Cox, P., et al. (2004). Regions of strong coupling between soil moisture and precipitation. *Science*, 305, 1138–1140.
- Kurc, S. A., & Small, E. E. (2004). Dynamics of evapotranspiration in semiarid grassland and shrubland ecosystem during the summer monsoon season, central New Mexico. *Water Resources Research*, 40, W09305.
- Kustas, W. P., Goodrich, D. C., Moran, M. S., Amer, S. A., Bach, L. B., Blanford, J. H., et al. (1991). An interdisciplinary field study of the energy and water fluxes in the atmosphere–biosphere system over the semiarid rangelands: Description and some preliminary results. *Bulletin of the American Meteorological Society*, 72, 1683–1705.
- Liu, Y., Bastidas, L. A., Gupta, H. V., & Sorooshian, S. (2003). Impacts of a parameterization deficiency on offline and coupled land surface model simulations. *Journal of Hydrometeorology*, 4, 901–914.
- Liu, Y., Gupta, H. V., Sorooshian, S., Bastidas, L. A., & Shuttleworth, W. J. (2004). Exploring parameter sensitivities of the land surface using a locally coupled land–atmosphere model. *Journal of Geophysical Research*, 109, 21101–21114.
- Liu, Y., Gupta, H. V., Sorooshian, S., Bastidas, L. A., & Shuttleworth, W. J. (2005). Constraining land surface and atmospheric parameters of a locally coupled model using observational data. *Journal of Hydrometeorology*, 6, 156–172.
- Mattikalli, N. M., Engman, E. T., Ahuja, L. R., & Jackson, T. J. (1998). Microwave remote sensing of soil moisture for estimation of profile soil property. *International Journal of Remote Sensing*, 19, 1751–1767.
- Mohanty, B. P., Shouse, P. J., Miller, D. A., & van Genuchten, M. T. (2002). Soil property database: Southern Great Plains 1997 hydrology experiment. *Water Resources Research*, 38, #1047.
- Moran, M. S., Peters-Lidard, C. D., Watts, J. M., & McElroy, S. (2004). Estimating soil moisture at the watershed scale with satellite-based radar and land surface models. *Canadian Journal of Remote Sensing*, 30, 805–826.
- Pellarin, T., Wigneron, J. -P., Calvet, J. -C., & Waldteufel, P. (2003). Global soil moisture retrieval from a synthetic L-band brightness-temperature data set. *Journal of Geophysical Research*, 108(D12), 4364. doi:10.1029/2002JD003086
- Peters-Lidard, C. D., Mocko, D. M., Santanello Jr., J. A., Tischler, M. A., Garcia, M. E. & Wu, Y. (submitted for publication). The Relative Roles of Soil, Land Cover, and Precipitation Uncertainty for Watershed-scale Soil Moisture Prediction in a Semi-arid Environment. *Water Resources Research*.
- Pitman, A. J. (2003). The evolution of, and revolution in, land surface schemes designed for climate models. *International Journal of Climatology*, 23, 479–510.
- Rawls, W. J., Brakensiek, D. L., & Saxton, K. E. (1982). Estimation of soil water properties. *Transactions of the American Society of Agricultural Engineers*, 1316–1320.
- Richards, L. A. (1931). Capillary conduction of liquids through porous mediums. *Journal of Applied Physics*, 1, 318–333.
- Robock, A., Luo, L. F., Wood, E. F., Wen, F. H., Mitchell, K. E., Houser, P. R., et al. (2003). Evaluation of the North American Land Data Assimilation System over the southern Great Plains during the warm season. *Journal of Geophysical Research*, 108(8846).
- Santanello, J. A., & Carlson, T. N. (2001). Mesoscale simulation of rapid soil drying and its implications for predicting daytime temperature. *Journal of Hydrometeorology*, 2, 71–88.
- Schaap, M. G., & Shouse, P. J. (2004). *Hydraulic data were collected and analyzed by Marcel G. Schaap, Univ. California at Riverside (SAHRA Science and Technology Center, NSF EAR-9876800) and Peter J. Shouse, GEBJ Salinity Laboratory (USDA-ARS), Riverside*.
- Schaap, M. G., Leij, F. J., & van Genuchten, M. T. (1998). Neural network analysis for hierarchical prediction for soil hydraulic properties. *Soil Science Society of America Journal*, 62, 847–855.
- Schumge, T. (1983). Remote sensing of soil moisture with microwave radiometers. *Transactions of the American Society of Agricultural Engineers*, 26, 748–753.
- Schumge, T. (1998). Applications of passive microwave observations of surface soil moisture. *Journal of Hydrology*, 213, 188–197.
- Schumge, T., Jackson, T. J., Kustas, W. P., Roberts, R., Parry, R., Goodrich, D. C., et al. (1994). Push broom microwave radiometer observations of surface soil moisture in Monsoon '90. *Water Resources Research*, 30, 1321–1327.
- Scott, R. L., Shuttleworth, W. J., Keefer, T. O., & Warrick, A. W. (2000). Modeling multiyear observations of soil moisture recharge in the semiarid American Southwest. *Water Resources Research*, 36, 2233–2247.
- Shamir, E., Imam, B., Gupta, H. V., & Sorooshian, S. (2005). Application of temporal streamflow descriptors in hydrologic model parameter estimation. *Water Resources Research*, 41, W06021.
- Sobieraj, J. A., Elsenbeer, H., & Vertessy, R. A. (2001). Pedotransfer functions for estimating saturated hydraulic conductivity: Implications for modeling storms flow generation. *Journal of Hydrology*, 251, 202–220.
- Soet, M., & Stricker, J. N. M. (2003). Functional behaviour of pedotransfer functions in soil water flow simulation. *Hydrological Processes*, 17, 1659–1670.

- Sun, W. Y., & Bosilovich, M. G. (1996). Planetary boundary layer and surface layer sensitivity to land surface parameters. *Boundary - Layer Meteorology*, 77, 353–378.
- Tischler, M., Gracia, M., Peters-Lidard, C., Moran, M. S., Miller, S., Thoma, D., et al. (2007). A GIS framework for surface-layer soil moisture estimation combining satellite radar measurements and land surface modeling with soil physical property estimation. *Environmental Modelling and Software*, 22, 891–898.
- Thoma, D. P., Moran, M. S., Bryant, R., Rahman, M., Holifield-Collins, C. D., Skirvin, S., et al. (2006). Comparison of four models to determine surface soil moisture from C-band radar imagery in a sparsely vegetated semiarid landscape. *Water Resources Research*, 42, W01418.
- Troen, I. B., & Mahrt, L. (1984). A simple model of the atmospheric boundary layer; sensitivity to surface evaporation. *Boundary - Layer Meteorology*, 37, 129–148.
- U.S. Department of Agriculture, Natural Resources Conservation Service (1994). *State Soil Geographic (STATSGO) database for Arizona*. State College, PA: Penn State University Earth Systems Science Center. http://www.essc.psu.edu/soil_info/index.cgi?soil_data&statsgo
- U.S. Department of Agriculture, Natural Resources Conservation Service (2006). *Soil Survey Geographic (SSURGO) Database for Cochise County, Arizona, Douglas-Tombstone Part*. Ft. Worth, TX: National Cartography and Geospatial Center. <http://www.nrcs.usda.gov/branch/ssb/products/ssurgo/>
- van de Griend, A. A., & O'Neill, P. E. (1986). Discrimination of soil hydraulic properties by combined thermal infrared and microwave remote sensing. *ESA Proceedings of the 1986 International Geoscience and Remote Sensing Symposium (IGARSS '86) on remote sensing: today's solutions for tomorrow's information needs, Vol. 2*(pp. 839–845).
- van Genuchten, M. Th. (1980). A closed-form equation for predicting the hydraulic conductivity of unsaturated soils. *Soil Science Society of America Journal*, 44, 892–898.